JOURNAL OF MORPHOLOGY 255:215–227 (2003)

Kinematic Model of Tyrannosaurid (Dinosauria: Theropoda) Arctometatarsus Function

Eric Snively* and Anthony P. Russell

Vertebrate Morphology Research Group, Department of Biological Sciences, The University of Calgary, Calgary, Alberta T2N 1N4, Canada

ABSTRACT We present a hypothesis of tyrannosaurid foot function termed the "tensile keystone model," in which the triangular central metatarsal and elastic ligaments dynamically strengthened the foot. The tyrannosaurid arctometatarsus, in which the central metatarsal is proximally constricted, displays osteological correlates of distal intermetatarsal ligaments. The distal wedge-like imbrication of tyrannosaurid metatarsals indicates that rebounding ligaments drew the outer elements towards the middle digit early in the stance phase, unifying the arctometatarsus under high loadings. This suggests increased stability and resistance to dissociation and implies, but does not demonstrate, greater agility than in large theropods without an arctometatarsus. J. Morphol. 255:215–227, 2003.

KEY WORDS: Tyrannosauridae; Theropoda; metatarsus; ligament; functional morphology

Integrative musculoskeletal studies constitute a promising approach for reconstructing the locomotor kinematics of extinct animals. While osteology is essential for investigating biomechanics of fossil and extant vertebrates, bones function as part of orchestrated systems incorporating muscles, tendons, and ligaments (Alexander et al., 1977; Maloiy et al., 1979; Nicholls and Russell, 1985; Pollock, 1991; Hutchinson, 2000; Rayfield et al., 2001). If bones of an extinct animal differ greatly from homologous elements in modern forms, rigorous consideration of unpreserved structures (Bryant and Russell, 1992; Witmer, 1995) is vital for functional reconstructions.

A particularly novel system of bones and unfossilized connective tissue is the arctometatarsus, a foot structure found only in several clades of Cretaceous theropod dinosaurs (Holtz, 1994, 1995). The foot of theropods has three weight-bearing digits, each with an elongate metatarsal between the ankle and the toe's phalanges bones that contact the substrate through subdigital pads. (Collectively, the metatarsals, or metacarpals, of the flat of the forefoot are referred to as the metapodium.) Normally, theropod metatarsals are roughly cylindrical. In the arctometatarsus, however, the third (central) metatarsal (MT III) is reduced to a narrow splint proximally (Fig. 1a,b) and is triangular in distal cross section (Lambe, 1917; Maleev, 1974; Coombs, 1978; Wilson and Currie, 1985; Holtz 1995). Proximally, the outer second and fourth metatarsals (MT II and MT IV) conceal MT III in anterior view (Fig. 1a) and encroach medially where MT III constricts towards the flat or posterior (plantar) surface of the foot (Fig. 1b) (Holtz, 1995).

In addition to the distinct shape of its elements, the arctometatarsus is longer relative to the upper leg than homologous elements of other theropods (Holtz, 1994). Modern terrestrial vertebrates with proportionally long lower limb elements are usually faster than less gracile relatives of similar mass (Hildebrand, 1988). While metatarsal length suggests that tyrannosaurids reached higher speeds than like-sized relatives (Holtz, 1994a), the question arises as to how the unique shape of MT III contributed to locomotion. Several workers have discussed possible modes of energy transmission within the arctometatarsus (Coombs, 1978; Wilson and Currie, 1985; Holtz, 1995; Snively and Russell, 2002), but none have addressed in detail the three-dimensional kinematics of the tyrannosaurid foot.

This article develops a functional model for the arctometatarsus that incorporates inferences of soft tissues. Our format follows the logical progression involved in developing and testing a complex hypothesis of locomotion: 1) We first introduce aspects of bone and connective organ function in large terrestrial vertebrates that suggest hypotheses of arctometatarsus morphology and action. 2) Our investigations and results test these proposals and lead inductively to a model of overall arctometatarsus function. 3) Because the model is emergent from the results, we present it in a separate section. 4) The subsequent discussion tests the model against mod-

Contract grant sponsors: NSERC (operating grant to APR), the Jurassic Foundation, the TMP Heaton Fund (to ES), University of Calgary Graduate Faculty Council Scholarships (to ES).

*Correspondence to: Eric Snively, Dept. of Biological Sciences, The University of Calgary, 2500 University Dr. NW, Calgary, Alberta T2N1N4, Canada. E-mail: esnively@ucalgary.ca

DOI: 10.1002/jmor.10059

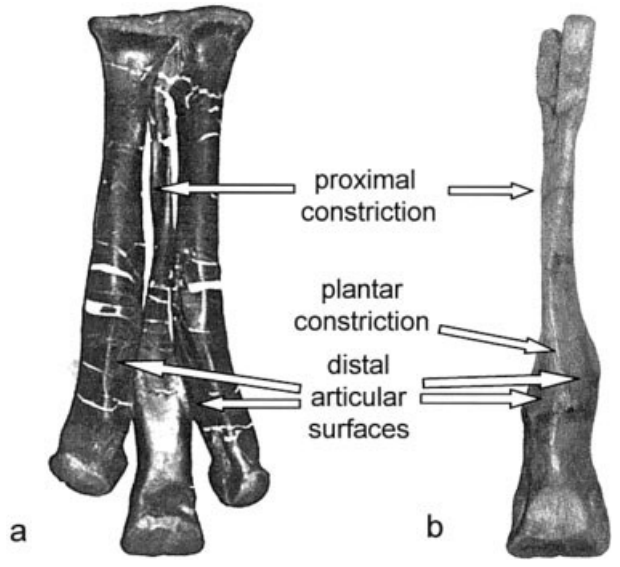

Fig. 1. The tyrannosaurid metatarsus. **a:** Left arctometatarsus of *Albertosaurus sarcophagus* (TMP 86.64.1) in anterior view. MT II and MT IV are displaced to show articular surfaces with MT III. **b:** Left MT III of *Gorgosaurus libratus* (MOR 657) in posterior view. For explanation of features, see text.

ern analogs and addresses implications of the proposed kinematics for tyrannosaurids.

The model therefore acts as a prism that focuses multiple lines of evidence into a coherent functional picture and a fulcrum over which morphological detail facilitates discussion of behavior. Our construction and application of the model exemplify the integrated approach necessary for reconstructing locomotion of extinct vertebrates.

Arctometatarsus as an Elastically Damped System

As with foot structures in modern animals, the arctometatarsus' role in tyrannosaurid locomotion hinged on the specific morphology of its bones and connective tissues. In vertebrates, tendons that join bone to muscle, and ligaments that connect bone to bone, transmit and dissipate locomotor forces acting on the skeleton (Hildebrand, 1988). Tendons and ligaments are variably elastic, depending on their relative proportions of collagen and elastin proteins (Alexander, 1988) and the magnitude and period of imposed loadings (Pollock, 1991). The bones of the arctometatarsus and its unmineralized tissues would have been elastic to some degree, but understanding its precise function depends, in part, on consideration of locomotor elasticity in modern vertebrates.

A number of studies have explicated the locomotor role of elastic ligaments and tendons and their interactions with associated bones. Elastic fore- and hindfoot connective elements store, return, and distribute footfall energies and forces. Ligaments of the feet of humans (Kerr et al., 1987; Alexander, 1988; Deane and Davies, 1995) and the wrists of horses (Rubeli, 1925) are noteworthy examples.

Ligaments absorb shock under specific physical conditions. Paradoxically, they display greater strength and resiliency when subject to high magnitude, sudden loadings, such as those incurred during rapid locomotion (Frank and Shrive, 1994). In animals of large body size, the extensibility of connective elements increases because their cross sectional area is lower relative to mass than ligaments and tendons of smaller animals (Pollock, 1991). The ligaments of large vertebrates store and return relatively more elastic strain energy, which increases locomotor efficiency and decreases strain energy transmitted to bones (Pollock, 1991). These conditions probably existed in adult tyrannosaurids, which ranged from two (Paul, 1988) to an upper estimate of eight tons (cross scaling of measurements from fragmentary metatarsals: University of California Museum of Paleontology, locality number V91181).

These considerations suggest that elastic mechanisms may have operated efficiently within the tyrannosaurid foot. Two contingencies are critical for assessing possible elastic functions: the type of connective tissues associated with the arctometatarsus and the freedom of movement between metatarsals. These factors lead to hypotheses of anatomy and movement necessary for erecting a comprehensive model of tyrannosaurid arctometatarsus function.

Prerequisites for Modeling Arctometatarsus Function: Reconstructing Soft Tissues and Intermetatarsal Displacement

Soft tissue reconstruction of extinct vertebrates entails comparison with extant relatives, ideally by bracketing the extinct taxon between modern, derived representatives of its clade and a more archaic living sister group (Bryant and Russell, 1992; Witmer, 1995). Although there are no extant arctometatarsalian theropods, unpreserved tissues are still inferable through broader phylogenetic comparison, mechanical considerations, and universal correlates of soft parts that are present on mineralized structures (Bryant and Seymour, 1990; Bryant and Russell, 1992).

Soft tissues leave consistent marks on bone, termed osteological correlates (Witmer, 1995), that are evident in both extant and fossil specimens. Ligament or tendon attachments display two primary correlates: rugosity, and rough or smooth faceted areas. Rugosity marks the location of Sharpey's fibers, mineralized collagen fibers within the bone that are continuous with fibers of the attaching connective element (Woo et al., 1987). Ligaments and tendons also attach through a gradient of fibrocartilage, mineralized fibrocartilage, and bone. These so-called direct insertions occur on

bone surfaces that are smooth and slightly concave (Doglo-Saburoff, 1929). Sutured or closely conforming bones invariably indicate ligament attachments, and more widely spaced adjacent facets may indicate tendon attachments (Gray and Goss, 1959).

Using these criteria we identified osteological correlates along intermetatarsal articular surfaces of large theropods. Ligaments would indicate passive elasticity and tendons would signify controlled function. Our study tested the following hypotheses: **H1:** Connective tissue scars on adjacent tyrannosaurid metatarsals indicate tendons. **H2:** Scar configuration was identical in tyrannosaurids and in the nonarctometatarsalian theropod, *Allosaurus fragilis*.

Freedom of movement between tyrannosaurid or *Allosaurus fragilis* metatarsals dictated the function of their associated ligaments or muscles. Therefore, this study sought to test hypotheses of possible intermetatarsal displacement. Preliminary observations of tyrannosaurid metatarsals, and the work of Wilson and Currie (1985) and Holtz (1995), suggested this hypothesized pattern of movement: **H3:** In the tyrannosaurid metatarsus, the distal end of MT III was free to move anteriorly to a small degree about a pivot point at the proximal end.

The proximal articulation between metatarsals, and their associated soft tissues, would constrain this potential displacement of MT III. Detailed consideration of both osteological and soft tissue anatomy was therefore necessary to test the hypotheses and come to a more complete understanding of tyrannosauruid arctometatarsus function.

Institutional abbreviations. MOR: Museum of the Rockies, Bozeman, Montana. IVPP: Institute of Vertebrate Paleontology and Paleoanthropology, Beijing, China. NMC: National Museum of Canada, Ottawa. PJC: Philip J. Currie, Royal Tyrrell Museum of Palaeontology, Drumheller, Alberta, Canada. TMP: Royal Tyrrell Museum of Palaeontology, Drumheller, Alberta. UCMP: University of California Museum of Paleontology, Berkeley, California. ROM: Royal Ontario Museum, Toronto, Ontario.

MATERIALS AND METHODS

For comparative purposes, specimens of large and small arctometatarsalian forms were examined at UCMP, MOR, and TMP. Metatarsal specimens of *Allosaurus fragilis* (MOR 693), and others at MOR and TMP, provided control representatives of the primitive condition for theropods. The specimens (Table 1) were sufficiently complete and well preserved for evaluation of osteological correlate position and/or resolution of possible intermetatarsal movement.

Assessment of metatarsus dynamics in tyrannosaurids entailed three related lines of inquiry: 1) We identified and measured osteological correlates of soft tissues in tyrannosaurids and *Allosaurus fragilis*. The proximity and complexity of joint surfaces tested whether the correlates indicated tendons or ligaments. 2) To ascertain the probable range of motion between elements in physical specimens, we manipulated casts of *Tyrannosaurus rex* metatarsals. 3) To evaluate intermetatarsal freedom of movement in other tyrannosaurids, we examined computed tomographic (CT) images of *Albertosaurus sarcophagus* and *Gorgosaurus libratus* metatarsals.

TABLE 1. Complete theropod metatarsus specimens examined

Taxon (arctometatarsus)*	Specimen number
*Albertosaurus sarcophagus**	MOR 657
*Albertosaurus sarcophagus**	TMP 81.10.1
*Albertosaurus sarcophagus**	TMP 86.64.1
*Chirostenotes pergracilis**	NMC 2367 (cast TMP 90.4.5)
*Daspletosaurus torosus**	MOR 590
*Gorgosaurus libratus**	TMP 94.12.602
*Elmisaurus sp.**	TMP 82.16.6
Ornithomimidae*	TMP 87.54.1
*Troodon formosus**	MOR
*Tyrannosaurus rex**	LACM 7244/23844) (cast TMP 82.50.7)
*Tyrannosaurus rex**	MOR 555
*Tyrannosaurus rex**	UCMP V80094-137539
Allosaurus fragilis	MOR 693
Allosaurus fragilis	ROM 5091 right (TMP casts)
Allosaurus fragilis	ROM 5091 left (TMP casts)
Deinonychys antirrhopus	MOR 793
Saurornitholestes langstoni	TMP 80.121.39
Sinraptor dongi	IVPP 10600 right (TMP casts)
Sinraptor dongi	IVPP 10600 left (TMP casts)

Assessment of Osteological Correlates

We ascertained the distribution and extent of osteological correlates on theropod metatarsals by identifying probable scars and measuring their areas. Likely correlates of soft tissues were identified on specimens in a satisfactory state of preservation, using the criteria of rugosity and delineated faceting outlined above. Surfaces had to be continuous with cortical bone that had not been taphonomically eroded, to avoid the potential of infilled spongy bone being mistaken for rugosity. Problematic degeneration was not present on the metatarsals chosen for area measurement.

We measured the area of the correlates only when their boundaries could be repeatably determined, but because soft tissues are not preserved, our techniques are subject to some inaccuracy. Our results, therefore, reflect the position and relative area of correlates more than their absolute extent.

Surface areas of osteological correlates were measured on specimens of *Albertosaurus sarcophagus* (MOR 657), *Allosaurus fragilis* (MOR 693), *Daspletosaurus torosus* (MOR 590), and *Tyrannosaurus rex* (MOR 555). The bones were wrapped in plastic cling film and attachment surface areas traced with a water-based marking pen. This technique facilitates area measurement of complexly contoured surfaces (Snively, 2000). The cling wrap was removed from the bone, pulled gently taut, and smoothed with a ruler. The markings were then retraced onto white paper and digitized. From these scans we determined the areas of the representations in cm^2 using NIH Object-Image for Macintosh.

The average of apparent attachment areas on adjacent bones was used to approximate the cross sectional area of intervening soft tissues. A disarticulated MT IV was not present in MOR 555. To estimate the areas on that bone, first the smaller ratio was found between MT IV and MT III in the other tyrannosaurids. This ratio was then multiplied by the corresponding MT III area in MOR 555.

Manipulation of *Tyrannosaurus rex* Casts

Casts of *Tyrannosaurus rex* metatarsals from the left foot of LACM 7244/23844 (TMP casts: 82.50.7) were positioned in proper articulation and wrapped with elastic bands. Rubber and polyester fiber bungy cords of low stiffness (0.75 meters long when untensed) were stretched and wound twice around the casts at

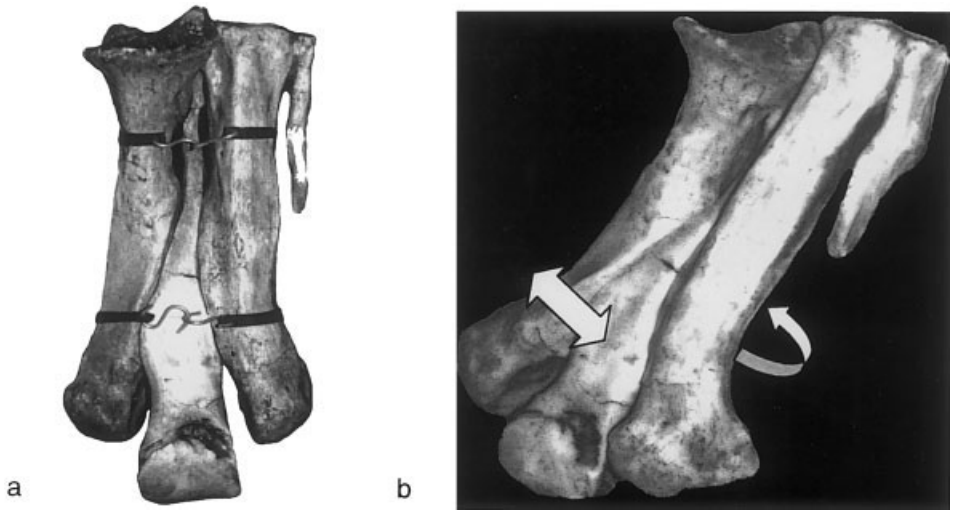

Fig. 2. Freedom of intermetatarsal movement determined in cast left metatarsus of *Tyrannosaurus rex* (LACM 7244/23844: cast TMP 82.50.7). **a:** Depiction of experimental setup. The metatarsus was wrapped in bungy cords to simulate a mechanism of elastic articulation. Larger cords than those employed in the manipulations shown for clarity. **b:** Arrows show general type of motion. MT II (left) slides in one plane, while MT IV (right) translates along an arc. MT IV was incorrectly restored proximally, but this has no effect on the interpretation of distal movement.

their proximal and distal ends, tightly enough for the ends to be secured together by their plastic hooks (Fig. 2a).

The casts were positioned and manipulated in several ways in order to investigate proximal and distal freedom of intermetatarsal movement.

Proximal movement. We placed the distal part of the metatarsus on a laboratory bench, alternately on its anterior and posterior surfaces, while we supported and manipulated the proximal end to assess possible intermetatarsal movement in this region.

Distal movement with the metatarsus in varying positions. We placed the proximal end of the metatarsus on the bench, with the posterior surface down, and supported the specimen by the third metatarsal. Rotating the metatarsus about its fixed proximal end revealed the passive displacement of MT II and MT IV relative to MT III, with the metatarsus in various positions, ranging from 0 to –90° from the horizontal. (Some of these positions are shown in the silhouettes in Fig. 5.)

Intermetatarsal displacement under simulated loading. The entire metatarsus was set on the bench. Taking care not to apply medial or lateral pressure, we pushed down on the dorsal surfaces of MT II and MT IV about 70% of their lengths from their proximal ends. We then lifted the distalmost portion of MT III. This showed the behavior of the outer metatarsals when a greater dorsally directed torque was applied to the distal part of MT III than to the distal ends of the other metatarsals.

CT Scanning of Tyrannosaurid Metatarsals

The methods described above apply to overall intermetatarsal movements. The topographical and likely functional complexity of the arctometatarsus compelled analysis of movement evident in cross sections at multiple transverse and longitudinal transects. As in clinical practice, the most common nondestructive technique for macroscopic paleontological sectioning is CT scanning.

In order to maximize the information from CT scanning and postprocessing visualization techniques, particular care was taken in specimen choice and preparation. TMP 94.12.602, a partial skeleton of *Gorgosaurus libratus* from the Dinosaur Park Formation (Late Campanian) of Dinosaur Provincial Park, Alberta, has a complete right metatarsus that has not been disarticulated taphonomically or through preparation. This specimen is undistorted and is intermediate in length and robustness between metatarsi of subadult *Albertosaurus sarcophagus* and adult *Tyrannosaurus rex*. For these reasons TMP 94.12.602 was deemed a suitable compromise for functional extrapolation to other tyrannosaurids.

The specimen was imaged at Children's Hospital and Health Center, San Diego. Prior to scanning the specimen was encased in plasticine to a depth of 2.5–4 cm to reduce the density gradient between the bone and the surrounding medium, and thus diffraction and scattering artifacts. Once prepared, TMP 94.12.602 was CT scanned at 140 kVp and 170 mA, technique settings that produce good readings from dense bone. The cross sectional data were reconstructed in three dimensions and these reconstructions were further sectioned, viewed, and printed in various orientations for study.

Additional CT scans of an *Albertosaurus sarcophagus* metatarsus (TMP 81.10.1) were performed at the Radiology Department of Foothills Hospital in Calgary, Alberta. A metal frame on the specimen caused diffraction artifacts, which we alleviated by adjusting contrast on the output images. Following this adjustment the shape of intermetatarsal articulation surfaces could be evaluated and possible relative movement determined in a given plane of section.

RESULTS

Osteological Correlate Reconstruction

The following intermetatarsal osteological correlates for soft tissues were identified. The surfaces of all but one scar (in *Allosaurus*) conform closely to the contours of the facing scar on the adjacent metatarsal. Rugosity indicating Sharpey's fibers occurs at proximal shaft-to-shaft articular surfaces in specimens of tyrannosaurids (Fig. 4a–c) and *Allosaurus* (Fig. 4d). Smooth articular facets extend the MT III-MT II articulation distally in *Allosaurus* (Fig. 4d). Indications of Sharpey's fibers are most striking along the distal articular surfaces between the shafts of MT II and MT III in large tyrannosaurids (Fig. 4a–c), but are not present at these locations in *Allosaurus* (Fig. 4d). A faceted distal MT III-MT IV articulation occurs in tyrannosaurids (Fig. 4a–c), but is entirely absent in *Allosaurus*, in which MT IV shows pronounced lateral angulation (Fig. 4d).

Proximal scars are subtriangular in all assessed theropods (Fig. 4), but in *Allosaurus* are long proximodistally relative to the length of the metatarsus. In all three tyrannosaurids distal articulations are

long and taper proximally. The average areas of adjacent distal scars are quite extensive in tyrannosaurids (Table 2). The average distal scar area exceeds the average proximal area by 1.5728 in *Daspletosaurus* (MOR 590), 1.4029 in *Albertosaurus* (MOR 657), and by 1.4666 in *Tyrannosaurus* (MOR 555; Table 2).

The intimate conformity of adjacent scars falsifies hypothesis H1, that tendons and muscles rather than ligaments were present between theropod metatarsals. Large distal osteological correlates on tyrannosaurid metatarsals, and their absence in *Allosaurus fragilis*, falsify the hypothesis (H2) that there were no marked differences in correlate morphology between the taxa.

Intermetatarsal Movement

1. Physical manipulation of *Tyrannosaurus rex* casts.

Proximal Movement. Proximally, displacement is greatly constrained by the hooked cross section of MT III and its articulation with anterolateral and posteromedial projections of MT II and MT IV, respectively (Fig. 2b).

Distal Movement. The distal portion of the third metatarsal is free to move anteriorly, corroborating hypothesis H3. When the anterior face of the metatarsus is parallel with the ground, only the distal elastic bands prevent this portion of MT III from pivoting towards the floor, with its center of rotation at the proximal clasped articulation.

When the posterior surface of the metatarsus faces the ground and the distal and proximal parts of MT III are fixed in position, the distal portions of MT II and MT IV slide ventrally and towards the centerline of MT III. MT II slides in a straight line along its articular surface with MT III. This contrasts with MT IV, which slides in more of an arc along its corresponding surface (Fig 2b).

Intermetatarsal displacement under simulated loading. When the posterior surface of the metatarsus again faces down, as just described, but with MT II and MT IV fixed proximally and distally, the same medial sliding motion occurs when the distal part of MT III is forced upwards and the bands stretch. As force is released from MT III, the bands recoil and the metatarsals return to their original articulation positions.

2. Freedom of movement inferred from *Gorgosaurus libratus* and *Albertosaurus sarcophagus* CT scans. These results show no gross variation in potential movement among the three metatarsi. The CT scanned specimens show the same proximal interlocking morphology as described for *Tyrannosaurus rex*. In *Gorgosaurus libratus* (TMP 94.12.602), cross sections along the metatarsus reveal that the distal articulation between MT II and MT III always slants ventromedially at the same angle (Fig. 3a). This indicates that displacement along this articulation will be in one plane, a motion identical to that possible in the physical model (see results for the cast manipulations above). By contrast, the MT IV-MT III articulations in the cross sections are not always in a straight line and the overall angle of the articulation varies with cross section. This corroborates the inference that motion along this articulation would transcribe an arc in the metatarsi of all three tyrannosaurids (Fig. 3b).

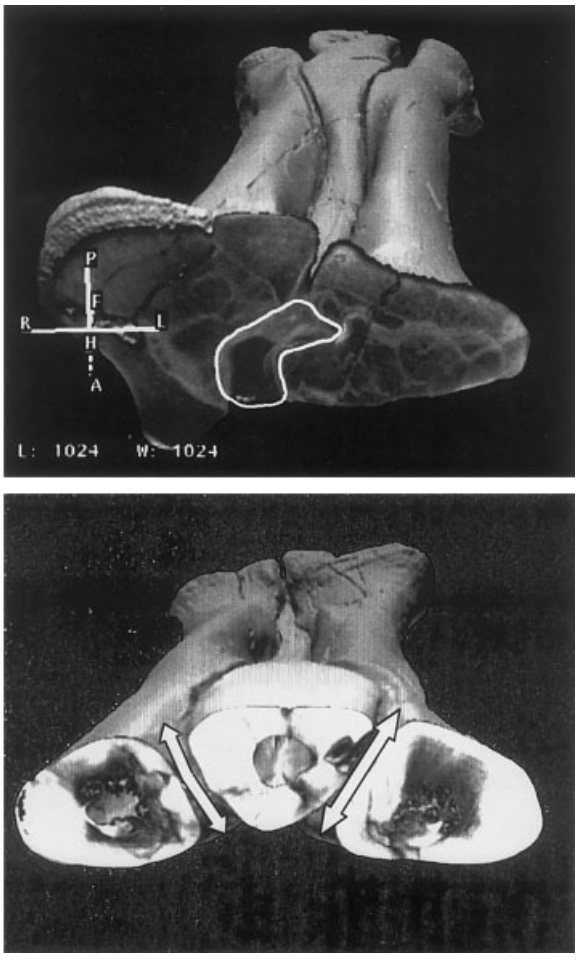

Fig. 3. Freedom of intermetatarsal movement of right *Gorgosaurus libratus* arctometatarsus (TMP 94.12.602), as determined through CT reconstructions. **a:** Proximal view near ankle. Proximal expansion of MT III at the exposed cross section is outlined in white. Anterior and posterior projections of the outer metatarsals constrained this portion of MT III from anteroposterior rotation. This partially clasped morphology functioned as a pivot point, enabling ligament-damped displacement of the distal third metatarsal. **b:** Distal view, with metatarsals cross sectioned 70% of their length from their proximal end. Arrows show a sliding motion possible between MT II and MT III, and a slight rotational motion between MT IV and MT III.

Kinematic Model of the Tyrannosaurid Arctometatarsus: The Tensile Keystone Hypothesis

The above results indicate that ligaments were the connective elements between adjacent tyranno-

TABLE 2. Surface areas of intermetatarsal osteological correlates in large theropods

	Specimen			
Area in cm^2	*Allosaurus fragilis* MOR 693	*Daspletosaurus torosus* MOR 590	*Albertosaurus sarcophagus* MOR 657	*Tyrannosaurus rex* MOR 555
Prox.: MT III-II:II	31.52	60.33	76.28	139.15
Prox.: MT III-II:III	72	56.49	61.47	116.01
Prox.: MT III-II:ave.	52.11	58.41	68.875	127.58
Prox: MT III-IV:IV	17.19	64.03	99.56	166.36
Prox.: MT III-IV:III	20.39	50.85	67.8	132.12
Prox: MT III-IV:ave.	18.79	57.44	83.68	149.24
Distal: MT III-II:II		99.91	114.15	220.48
Distal: MT III-II:III		93.76	107.09	168.46
Distal: MT III-II:ave.		96.835	110.62	194.47
Distal: MT III-IV:IV		85.1	99.66	203.87
Distal: MT III-IV:III		85.64	107.14	219.17
Distal: MT III-IV:ave.		85.37	103.4	211.52
Ratio of average correlate areas: distal/proximal	0.00*	1.5728	1.4029	1.4666

*No distal correlates.

Osteological correlate areas in Allosaurus fragilis (MOR 693), Albertosaurus sarcophagus (MOR 657), Daspletosaurus torosus (MOR 590), and Tyrannosaurus rex (MOR 555). Areas are in cm^2. Areas of proximal correlates are designated as "Prox.," and distal correlates as "Distal." The last row shows the ratios of distal to proximal areas. The convention for naming the metatarsals and their respective correlate areas is as follows: MT III-II:II = articulation between Metatarsals III and II; surface of Metatarsal II. MT III-II:III = articulation between Metatarsals III and II; surface of Metatarsal III. MT III-II:ave = average area of corresponding articular surfaces on Metatarsals III and II. MT III-IV:IV = articulation between Metatarsals III and IV; surface of Metatarsal IV. MT III-IV:III = articulation between Metatarsals III and IV; surface of Metatarsal III. MT III-IV:ave = average area of corresponding articular surfaces on Metatarsals III and IV.

saurid metatarsals and reveal degrees of freedom and constraint for tyrannosaurid intermetatarsal movement through the ground contact (stance) phase of the step cycle (Figs. 5–6). These considerations suggest the following pattern of intermetatarsal kinematics when the foot was in contact with the substrate.

1. The foot pads ventral to the phalanges would contact the substrate initially (Fig. 5b). Ground-reaction forces would transfer to the metatarsals first across the metatarsophalangeal joints and then to the portions of the foot pad ventral to the respective metatarsals. This sequence has been corroborated through observations of domestic chickens and ostriches.
2. Because metatarsal III (MT III) is longest, the ground-reaction force would act upon the longest moment arm from the mesotarsal to the phalangeal joints. This torque differential would displace MT III anterodorsally relative to MT II and IV (Fig. 5b,c). Anteroposterior rotation of the proximal portion of MT III, as suggested for the small arctometatarsalian *Troodon inequalis* (Wilson and Currie, 1985), was not possible in tyrannosaurids (Fig. 3a). Instead, the clasped proximal articulation between metatarsals would serve as a pivot point for distal rotation of MT III (Figs. 5b–e, 6b).
3. Crucially, forces from this differential loading and displacement pattern would stretch distal intermetatarsal ligaments (Fig. 5b). Upon rebound (Fig. 5c,d), the angulation of metatarsals, and orientation of ligaments, would draw the distal portion of the lateral metatarsals together ventrally and towards the midsagittal plane of the third metatarsal (Fig. 6).
4. Forces from anterior displacement of MT III, which stretched intermetatarsal ligaments in the manner described, would decrease as the metatarsus became vertical and parallel with the ground-reaction force. In this position, ground-reaction loadings on MT III would be transferred laterally via MT II and MT IV to the condyles of the astragalus (Wilson and Currie, 1985; Holtz, 1995). Tensile loading on intermetatarsal ligaments would mediate the energy transfer (Fig 5e').

This pattern of movement has several implications. The distal arctometatarsus would become more unitary under high initial footfall loadings (Fig. 6). In effect, the outer metatarsals would "splay" away from the center midline of MT III only as forces lessened, returning to their unloaded configuration.

Upon strongly oblique or torsional footfalls, ligaments and the imbricate distal cross section of the metatarsals (Fig. 7) would strongly arrest interelement shear. Potentially damaging torsion of the metatarsus would be induced during abrupt turns in which torque was insufficient to overcome friction between the foot pad and the ground. The plantar angulation between metatarsals would ensure that torsional loadings were transferred from one meta-

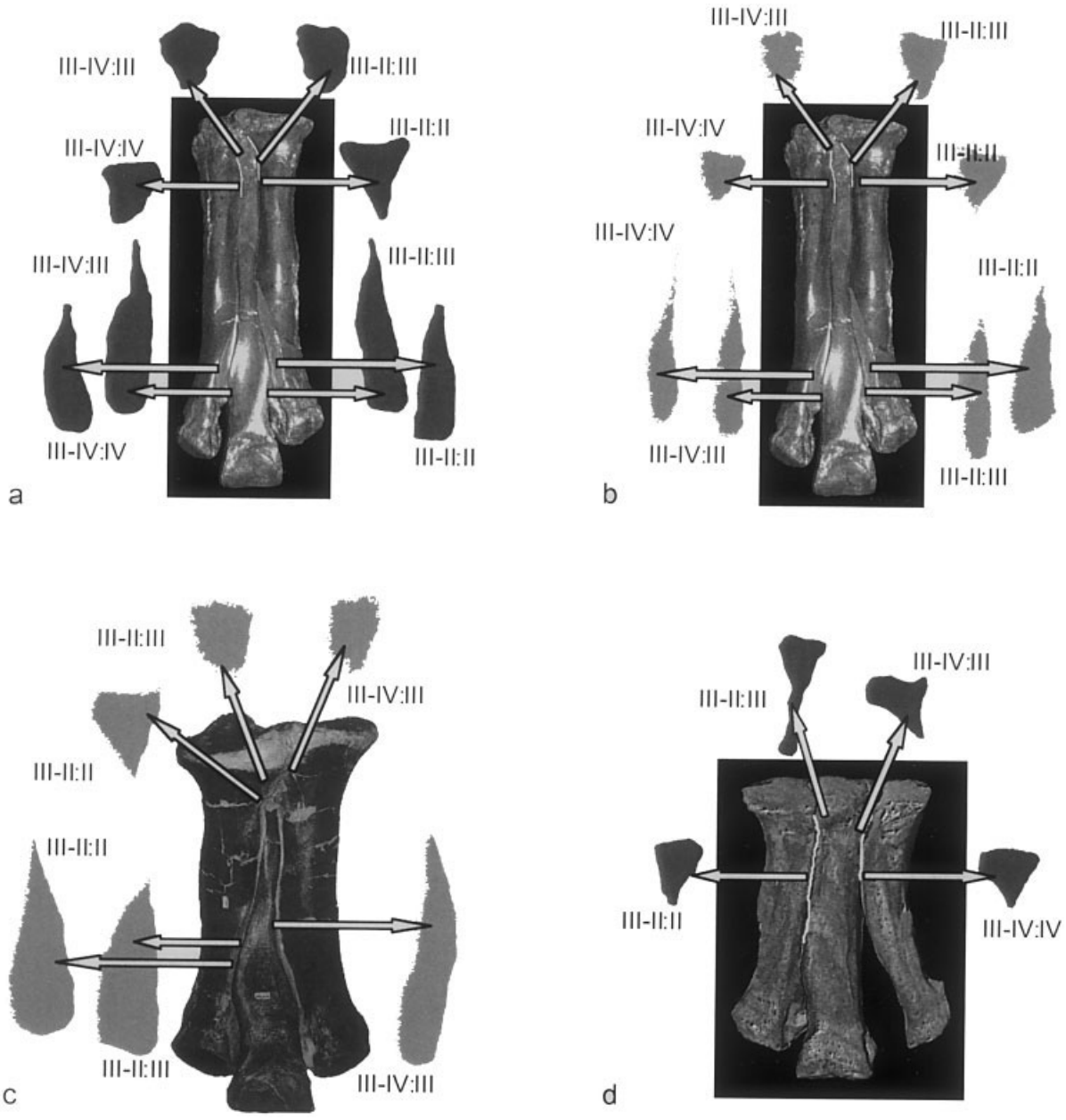

Fig. 4. Osteological correlates on metatarsi of tyrannosaurids and *Allosaurus fragilis*. Gray-filled tracings show the shape and size of correlates; arrows and correlate designations from Table 2 indicate the corresponding metatarsal for each scar. For clarity, correlates are mapped onto articulated specimens, with scar locations marked. *Albertosaurus* and *Daspletosaurus* correlates are shown on an articulated right metatarsus of *Albertosaurus sarcophagus* (TMP 81.10.1), with MT III recessed to show distal correlates on outer metatarsals. Correlates for the *Tyrannosauurs* and *Allosaurus* specimens are mapped onto left articulated metatarsi (MOR 555 and ROM specimen, respectively). **a:** *Albertosaurus sarcophagus* MOR 657: left. **b:** *Daspletosaurus torosus* MOR 590: right. **c:** *Tyrannosaurus rex* MOR 555: right. **d:** *Allosaurus fragilis* MOR 693: left.

tarsal to the next (Fig. 7a) and would obviate anteroposterior shear. The large cross sectional area and consequent stiffness of the distal intermetatarsal ligaments (Figs. 4, 7b) would check lateral shearing components introduced by torsion.

We propose the appellation "tensile keystone model" for these kinematics. Although the loading regimes are inverted, one can think of the distal part of MT III and its ligaments as analogous to the keystone of a Roman arch, in which the central element imparts stability to the entire structure.

DISCUSSION

Comparisons with Modern Analogs: Implications of Soft Tissue Scars

The results indicate that correlates of soft tissues present on large theropod metatarsals were liga-

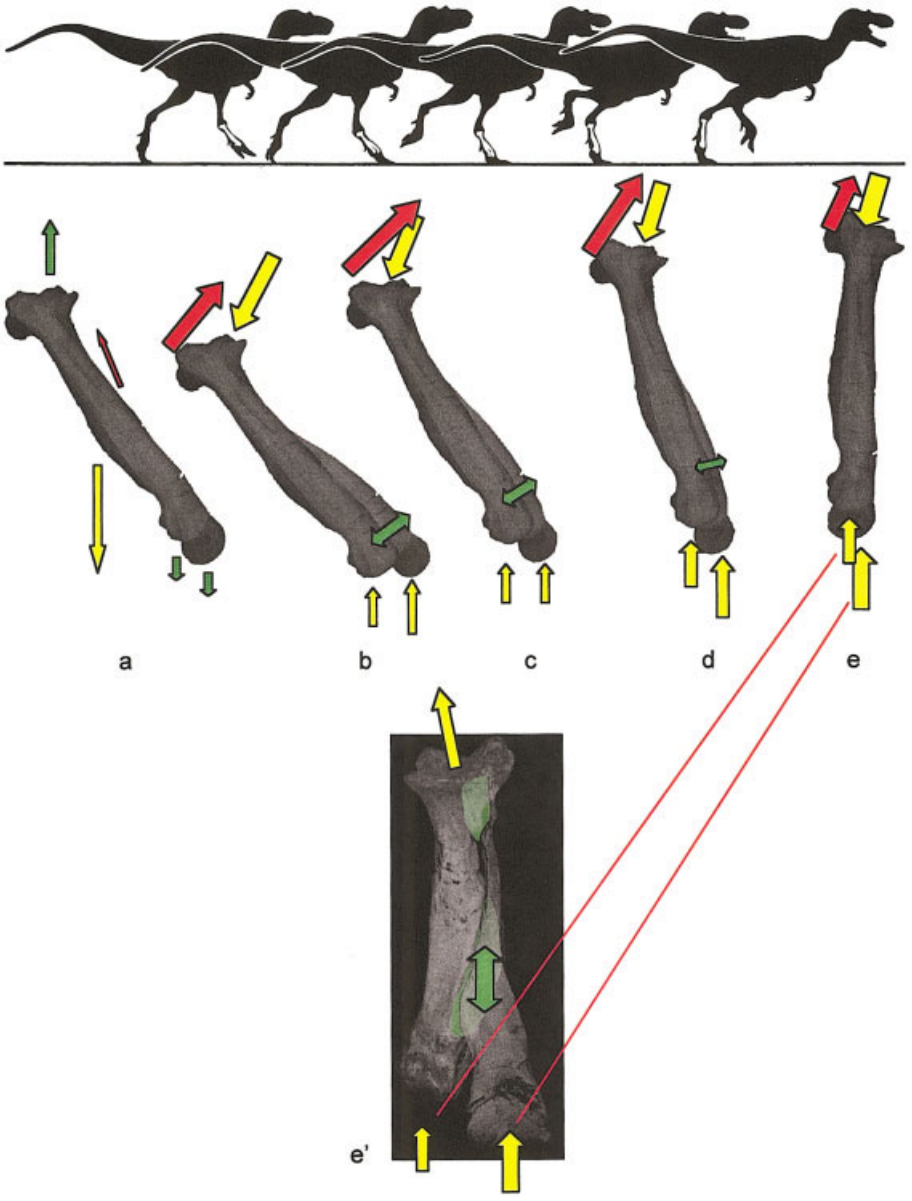

Fig. 5. Step sequence of *Gorgosaurus libratus* metatarsus in lateral view, showing forces acting on bones and ligaments during linear locomotion. Silhouettes depict the tyrannosaurid at appropriate locomotory stages. Vector sizes represent relative magnitude of forces; yellow, resultants of compressive force on bone; red, muscle forces; green, tensile forces on ligaments. Compressive loading on MT III stretches stiff ligament fibers oriented along the long axis of the metatarsus. The ligaments transmit this force to MT II, which is pulled dorsomedially. MT II thus transmits its own compressive loadings, and those of MT III, across the mesotarsal joint. MT IV also transfers loadings from MT III, but is omitted here for clarity. **a:** Prior to footfall, ligaments suspend metatarsus and toes; flexor muscles draw toes forward. **b–e:** Differential forces on metatarsal III and outer metatarsals stretch intermetatarsal ligaments, which return elastic strain energy. For clarity, displacement of MT III is exaggerated and articulating bones and bending components are omitted. **e':** MT II (left element) and MT III (right element), from a left metatarsus of *Tyrannosaurus rex* (LACM 7244/23844: cast TMP 82.50.7). Green indicates ligament scars on MT II below and MT III above, sloping away from the plane of the figure. The portion of either bone that lies anterior to the other in a given region is rendered transparent.

ment scars. In extant vertebrates, muscles and tendons do not normally attach on facing medial and lateral surfaces of closely joined, weight-bearing elements. The closely adpressed articular surfaces of theropod metatarsals argue against the presence of muscles; negligible fiber lengths would prevent the muscles from performing positive work.

In contrast to the rarity of muscles and tendons, proximal ligaments are common between metatarsals (Kerr et al., 1987; McGregor, 2000). Among squamates, ligaments with oblique distolateral angulation are present in the metacarpus and metatarsus of lizards (Landsmeer, 1981; McGregor, 2000). The presence of oblique deep ligaments in lizards does not allow bracketing for homologous ligaments within the theropod metatarsus. However, it does show that ligaments of similar angulation to that hypothesized for the arctometatarsus are mechanically feasible.

The strong inference of osteological correlates as ligament scars corroborates the tensile keystone model. However, possible extant analogs can potentially falsify the hypothesis if their behavior contradicts expectations of bone–ligament function.

Comparisons With Modern Analogs: Horse Wrists and the Feet of Cursors

Several aspects of the tensile keystone model, and Holtz's (1995) complementary hypothesis of energy

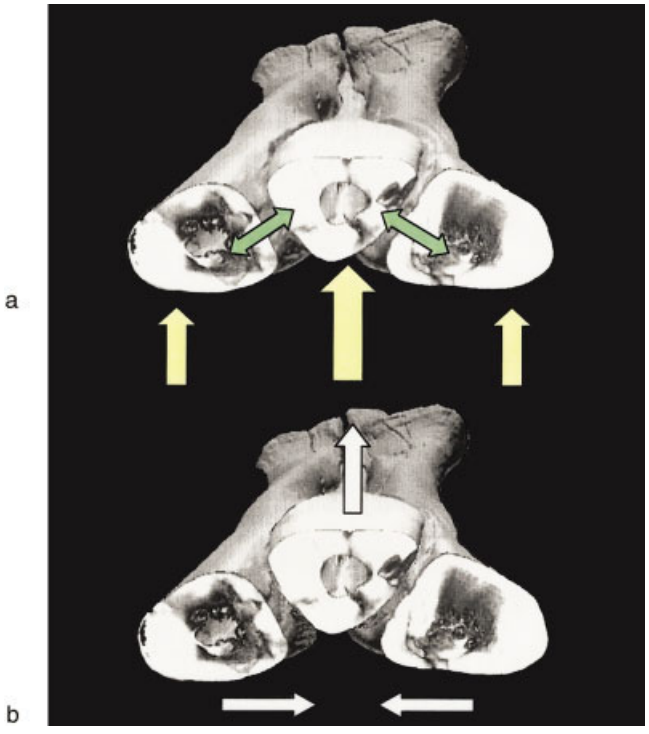

Fig. 6. CT reconstructions of right *Gorgosaurus libratus* arctometatarsus, showing tensile keystone model of stance phase kinematics. Vector sizes represent relative magnitudes of force. **a:** Corresponds to Figure 5b. When the foot pads beneath the metatarsals come into full contact with the substrate, the longer central metatarsal III (MT III) is displaced dorsally (white arrow) by ground-reaction forces greater than those on MT II and MT IV (yellow arrows). This force differential imposes tension on intermetatarsal ligaments (green arrows). **b:** Corresponds to Figure 5c. Ligaments draw outer metatarsals towards each other (white arrows), as elastic strain energy stored in the ligaments is returned.

transference, conform remarkably with the functional morphology of the wrist (carpus) of horses. For example, the horse carpus attains high aggregate surface area between individual carpal bones, with the development of wedge-like amphiarthroses and a full complement of elements (Figs. 8a). High surface area decreases pressure impinging on any one carpal surface and pressure transmitted to the radius (Bourdelle and Bressou, 1972). In the arctometatarsus distal ligaments and the distal plantar angulation of elements increased total articulation surface area and ligament cross section (Fig. 4; Table 2), which probably conferred a similar benefit.

Rubeli (1925) demonstrated an additional advantage to the wedge-and-ligament morphology of the horse carpus, which has dorsal ligaments on the anterior surface and deep interosseous ligaments between carpals (Fig. 8a,b). Interosseous ligaments transduce sudden compressive loadings into a collectively longer period of elastic loadings, reducing the rate of strain. Ligaments in the arctometatarsus may have mediated the transfer of compressive forces across the ankle joint (to the astragalar condyles: Holtz, 1995) in a similar manner (Fig. 8c). Horse interosseous carpal ligaments stretch and rebound under high momentary loadings (Fig. 8b) (Rubeli, 1925) and the same would be expected for tyrannosaurid intermetatarsal ligaments (Fig. 8c) (Frank and Shrive, 1994).

The shear- and torsion-resisting aspects of the tensile keystone model also find analogs in the equine wrist. Wedge-like articulations generally resist shear between horse carpals (Boening, 1981). A triangular sagittal projection of the distal radius (Figs. 1c, 8) buffers ad- or abductional torsion (Poplewski, 1936). Faces of this projection act as stop facets (Yalden, 1971) against dorsomedial or dorsolateral rotation of the radial and intermediate carpals. Tyrannosaurid metatarsals and metapodial ligaments would function analogously by arresting torsional forces. Unlike the horse morphology, how-

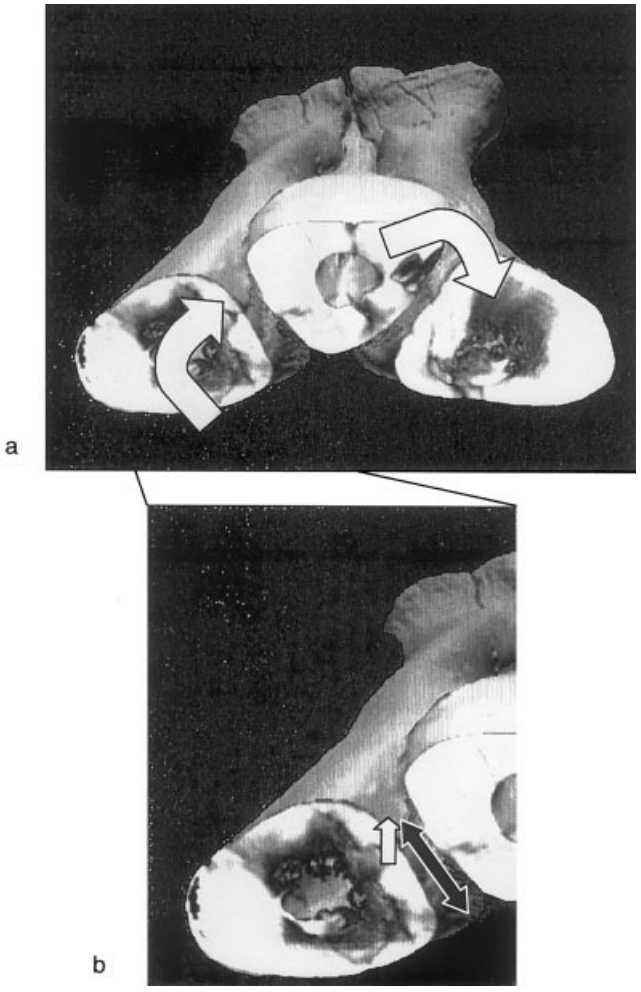

Fig. 7. Torsional loading transfer within the *Gorgosaurus libratus* arctometatarsus (right: TMP 94.12.602). Arrows reflect force directions, but not relative force or displacement magnitudes. **a:** Torsion (white arrows) translated into compression impinging on adjacent metatarsal. **b:** Anterior components (white) offset from compressional translation would cause anterolaterally directed tension on intermetatarsal ligaments (gray).

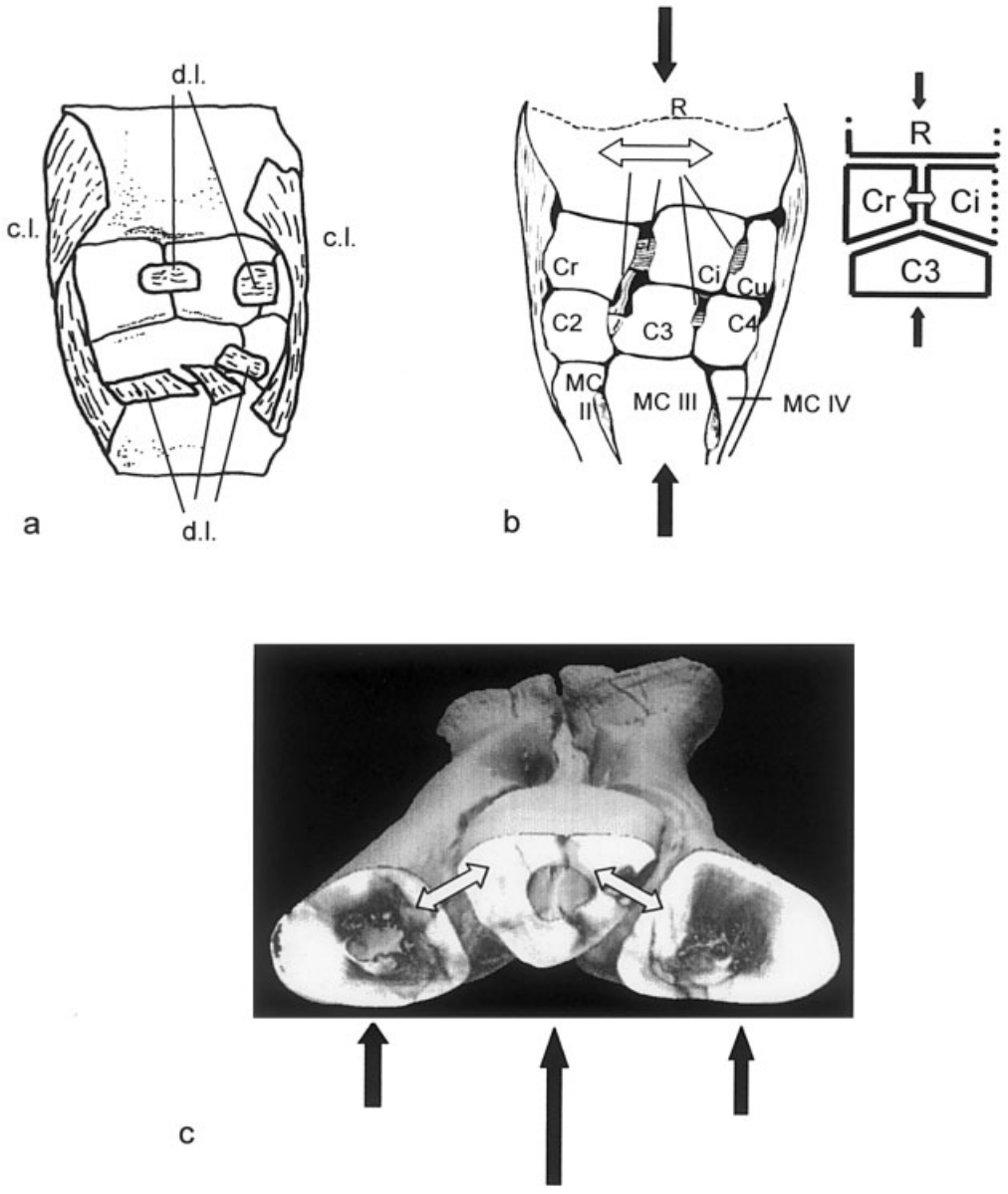

Fig. 8. Comparison of loading regimes on bones and ligaments of the equid carpus and tyrannosaurid arctometatarsus. Tyrannosaurid intermetatarsal ligaments are analogous in position and function with the interosseous ligaments of the horse carpus. **a:** Anterior view of left horse carpus, showing wedge-like articulations between carpals and dorsal ligaments (dl) connecting them. Modified from Sisson and Grossman (1953). **b:** Diagrammatic midfrontal section through horse carpus shows stretching (white arrow) of deep interosseous ligaments upon compressive loadings (black arrows) of the wrist. Inset shows how compression on the radius (R) and third carpal (C3) causes the wedge-like dorsal surface of C3 to laterally displace the radial and intermediate carpals (Cr and Ci). A portion of the compressive force is translated into tensile loading (white arrows) on the interosseous ligament between Cr and Ci. Modified from Sisson and Grossman (1953). **c:** A plurality of ground-reaction loadings (black arrows) is imposed on the tyrannosaurid MT III, the central element in this diagram. Loading differentials between MT III and MT II and MT IV, respectively, cause tensile stresses on intermetatarsal ligaments (white arrows).

ever, these elements would primarily buffer torsion about the midsagittal axis (Figs. 1c, 8).

A more fundamental distinction between horse intercarpal and tyrannosaurid intermetatarsal ligament function lies in the initial loading regime upon footfall. The horse third metacarpal, the single weight-bearing element of the anterior metapodium, transfers compressive forces directly to the carpus (Figs. 1c, 8) (Rubeli, 1925). The carpus acts as a shock absorber for the compressive ground-reaction force. Under the tensile keystone model, dorsally directed components of the ground-reaction force load the three tyrannosaurid metatarsals unevenly (Figs. 5, 6, 8c). The third metatarsal is displaced anteriorly relative to MT II and MT IV; differential forces stretch intermetatarsal ligaments, which rebound elastically to draw the distal portions of the outer metatarsals together. This resulting distal

unification does not have a counterpart in the horse carpus, although a long snap ligament absorbs shock to the entire forefoot.

Tensile keystone dynamics may explain the benefit of retention of multiple elements in the tyrannosaurid arctometatarsus, which contrasts with fused metapodia in ratites and in horses, bovids, cervids, camelids, giraffids, and other ungulates. A system of three bones and elastic ligaments may have imparted resilience and enhanced collective strength, properties diminished in a single metapodial element. The retention of multiple metatarsals as a stay against torsion may be paralleled in the Patagonian cavy, an agile cursorial rodent whose mesaxonic metapodia subtend an arch (pers. obs.). However, the metatarsals of the cavy lack the extremity of plantar angulation seen in the arctometatarsus, so the analogy is superficial and remains to be tested biomechanically.

A dynamically robust metatarsus is perhaps selectively logical in tyrannosaurids, which are much larger than most classically cursorial (fast-running) ratites and ungulates. Giraffes are potentially problematic to this view, because they are closer in mass to tyrannosaurids and have fused metapodia. As quadrupeds, giraffes have the advantage of lower loadings on the metapodia when trotting because two limbs share the load, although forces on each metapodium when galloping would be higher because the duty factor is low (Alexander et al., 1977). Giraffes are also not as fast as might be expected from the extreme elongation of their limbs. The energy-absorbing metapodium of adult tyrannosaurids conceivably enabled them to outmatch giraffes in certain maneuvers or in linear speed, but such transtemporal comparisons are unproductively speculative.

The preceding discussion derives from an adaptationist perspective (Gould and Lewontin, 1979). In contrast, phylogenetic and developmental contingency, rather than adaptation (Gould and Vrba 1982), also helps to explain the persistence of separate elements in the tyrannosaurid metatarsus. Giraffids, including the modern giraffe and okapi, inherited their metatarsal morphology from less specialized artiodactyls. Ratite birds inherited fused metatarsals from their avian ancestors and selective pressures for cursoriality need not be invoked to explain their ankylosed morphology. With this caveat in mind, we now explore arctometatarsus function in the context of performance and phylogeny.

Comparative Phylogenetic and Functional Implications

The tensile keystone model differs from kinematics likely evident in the foot of *Allosaurus* or other theropods with three largely autonomous metatarsals. As with humans (Kerr et al., 1987), footfall loadings would cause their outer metatarsals to splay beyond their resting orientation, essentially spreading the foot apart. During deviations from linear locomotion, metatarsals would experience increased bending loads individually, rather than as part of a single structure, as predicted for the arctometatarsus (Fig. 6). Broad-footed theropods are not uniform in metatarsus morphology (Snively, 2000). None of these animals, however, display plantar constriction of MT III consistent with distal unification of the metatarsals, which would occur in the arctometatarsalian pes under the tensile keystone model.

The probable multiple origin of the arctometatarsus (Sereno, 1999; Holtz, 2000) suggests it was not a legacy morphology, which was simply retained with no contemporary utility. Instead, it may have conferred a selective or performance benefit. Developmental and immediate functional advantages are not mutually exclusive. The correlation between a constricted third metatarsal and proportionally long metatarsus (Holtz, 1995) suggests a developmental correspondence. Unfortunately, developmental hypotheses of this type are tenuously ad hoc. Perhaps the ontogenetic program for lengthened separate metatarsals reciprocally invoked proximal and plantar constriction of MT III in coelurosaurs, but tensile keystone dynamics evince more for the tyrannosaurid arctometatarsus than simply a developmental contribution to the lengthened foot.

Another possibility is that the tensile keystone morphology conferred heightened agility for a given body mass. As such, the arctometatarsus may have been broadly analogous to the stiffened tails of dromaeosaurid coelurosaurs (Ostrom, 1969), which have been suggested as dynamic stabilizers. Because there was no anteriorly propulsive component to the elastic rebound of ligaments, third metatarsal constriction did not directly avail increased speeds. Instead, the unifying and shear-resisting properties of the arctometatarsus may have absorbed forces involved in linear deceleration, lateral acceleration, and torsion more effectively than the feet of other theropods. These forces are limiting factors to combat performance in humans (Snively: pers. obs. in open hand and weapons sparring) and the arctometatarsus may have imparted momentarily excessive construction (Gans, 1974) for selectively crucial behaviors, such as predation or escape.

However, while the potential may have been present the employment and utility of increased agility in tyrannosaurids are no more directly testable than ontogenetic hypotheses. As with the evolutionary correlation between cursoriality and pursuit predation in theropods (Carrano, 1998), alternate hypotheses must be explored. In addition, the tensile keystone model cannot be taken to indicate that tyrannosaurids behaved more dynamically than *Allosaurus*. Whether tyrannosaurids used the potential for higher maneuverability during prey capture, and how close these animals operated to safety limits, are untestable by observation. Conse-

quently, definitive statements about comparative agility in theropods are premature. However, the tensile keystone model demonstrates, in one aspect of hindlimb function, potential benefits to agility in large arctometatarsalians.

CONCLUSION

Although the sample size of large, rare fossil organisms is notoriously small (Kemp, 1999), the morphological evidence outlined above suggests significant dynamic differences between the metatarsi of tyrannosaurids and other large theropods. The tensile keystone model proposes that orientation and extent of ligaments in the arctometatarsus increased resistance to dissociation over that of other theropods, and yet allowed resiliency otherwise diminished in metapodia reduced to a single element, as in extant ratites, horses, or giraffids. These subhypotheses must be tested thoroughly in order to falsify or augment the overall model. Promising methods for further elucidating tyrannosaurid arctometatarsus function include dynamic computer modeling, quasi-static modeling (Hutchinson, 2000), and finite element analysis of strain in the tyrannosaurid foot (Snively and Russell, 2002).

ACKNOWLEDGMENTS

Donna Sloan prepared the silhouettes in Figure 5. We thank Greg Erickson, Carole Hickman, Ross Nehm, Matt Vickaryous, Kevin Padian, Philip Currie, and particularly Lisa McGregor and John Hutchinson for reviewing this article in various iterations. We also thank two anonymous reviewers, whose comments fundamentally improved the manuscript. Children's Hospital and Health Center of San Diego provided vital CT scanning and 3D reconstruction services. Foothills Hospital of Calgary provided additional CT scanning. We especially thank J. Howard Hutchison, Mark Goodwin, Patricia Holroyd, John R. Horner, Tim Schowalter, Andrew Neuman, and Jackie Wilkie for access to specimens in their care.

LITERATURE CITED

Alexander RM. 1988. Elastic mechanisms in animal movement. Cambrdge, UK: Cambridge University Press.

Alexander RM, Langman VA, Jayes AS. 1977. Fast locomotion of some African ungulates. J Zool Lond 183:291–300.

Boening KJ von. 1981. Hyperextensionfolgen im Karpalgelenksbereich. Der Praktische Tierzart 7:606–608.

Bourdelle E, Bressou C. 1972. Anatomie Regionale des Animaux Domestiques. I. Equides: Cheval – Ane – Mulet. Fascicule III. Region thoracique. Membre anterieur ou thoracique. Paris: JB Baillere et Fils.

Bryant HN, Russell AP. 1992. The role of phylogenetic analysis in the inference of unpreserved attributes of exinct taxa. Philos Trans R Soc Lond B 337:405–418.

Bryant HN, Seymour KL. 1990. Observations and comments on the reliability of muscle reconstruction in fossil vertebrates. J Morphol 206:109–117.

Carrano MT. 1998. Locomotion in non-avian dinosaurs: integrating data from hindlimb kinematics, in vivo bone strains, and bone morphology. Paleobiology 24:430–469.

Coombs WP Jr. 1978. Theoretical aspects of cursorial adaptations in dinosaurs. Q Rev Biol 53:393–418.

Deane NJ, Davies AS. 1995. The function of the equine carpal joint: a review. N Z Vet J 47:45–47.

Doglo-Saburoff B. 1929. Uber Ursprung und Insertion der Skeletmuskeln. Anat Anz 68:80–87.

Frank CB, Shrive NG. 1994. Ligaments. In: Nigg BM, Herzog W, editors. Biomechanics of the musculo-skeletal system. Chichester, UK: John Wiley & Sons.

Gans C. 1974. Biomechanics: an approach to vertebrate biology. Philadelphia: Lippincott.

Gould SJ, Lewontin RC. 1979. The spandrels of San Marco and the Panglossian paradigm: a critique of the adaptationist programme. Proc R Soc Lond B 205:581–898.

Gray H, Goss HC. 1959. Anatomy of the human body, 27 ed. Philadalphia: Lea and Febiger.

Hildebrand M. 1988. Analysis of vertebrate structure. Chichester, UK: John Wiley & Sons.

Holtz TR Jr. 1995. The arctometatarsalian pes, an unusual structure of the metatarsus of Cretaceous Theropoda (Dinosauria: Saurischia). J Vert Paleontol 14:480–519.

Holtz TR Jr. 1994. The phylogenetic position of the Tyrannosauridae: implications for theropod systematics. J Paleontol 68: 1100–1117.

Holtz TR Jr. 2000. A new phylogeny of the carnivorous dinosaurs. Gaia 15:5–61.

Hutchinson JR. 2000. Hindlimb function in extinct theropod dinosaurs: integrating osteological, soft tissue, and biomechanical data. J Vert Paleontol 25(Suppl to 3):50A.

Kemp TS. 1999. Fossils & evolution. Oxford: Oxford University Press.

Kerr RF, Bennett MB, Bibby SR, Kester RC, Alexander RM. 1987. The spring in the arch of the human foot. Nature 325: 147–149.

Lambe LW. 1917. The Cretaceous theropodous dinosaur *Gorgosaurus*. Mem Geol Surv Can 100:1–84.

Landsmeer JMF. 1981. Digital morphology in *Varanus* and *Iguana*. J Morphol 168:289–295.

Maleev EA. 1974. Giant carnivorous dinosaurs of the family Tyrannosauridae. Sovm Sov-Mong Paleontol Exped Trudy 1:131–191.

Maloiy GMO, Alexander RM, Njau R, Jayes AS. 1979. Allometry of the legs of running birds. J Zool Lond 187: 161–167.

McGregor L. 2000. Locomotor morphology of *Anolis*: comparative investigations of the design and function of the subdigital adhesive system. Thesis, University of Calgary.

Nicholls EL, Russell AP. 1985. Structure and function of the pectoral girdle and forelimb of *Struthiomimus altus* (Theropoda: Ornithomimidae). Palaeontology 28:638–667.

Ostrom JH. 1969. Osteology of *Deinonychus antirrhopus*, an unusual theropod from the Lower Cretaceous of Montana. Bull Peabody Mus Nat Hist 30:1–165.

Paul GS. 1988. Predatory dinosaurs of the world. New York: Simon & Schuster.

Pollock C. 1991. Body mass and elastic strain in tendons. Thesis, University of Calgary.

Poplewski R von. 1936. Biomechanik des Carpus bei Equiden. Anat Anz 81:333–341.

Rayfield JE, Norman DB, Horner CC, Horner JR, Smith PM, Thomason JJ, Upchurch P. 2001. Cranial design and function in a large theropod dinosaur. Nature 409:1033–1037.

Rubeli O von.1925 Zur Anatomie und Mechanik des Karalgelenks der Haustiere, Spezielle des Pferdes. Schweizer Archiv fur Tierheilkunde 67:427–432.

Sereno PC. 1999. The evolution of dinosaurs. Science 284:2137–2147.

Sisson S, Grossman JD. 1953. The anatomy of domestic animals. Philadelphia: WB Saunders.

Snively E. 2000. Functional morphology of the tyrannosaurid actometatarsus. Thesis, University of Calgary.

Snively E, Russell AP. 2002. The tyrannosaurid metatarsus: bone strain and inferred ligament function. Senck. Lethaea 82:35–42.

Wilson MC, Currie PJ. 1985. *Stenonychosaurus inequalis* (Saurischia: Theropoda) from the Judith River (Oldman) Formation of Alberta: new findings on metatarsal structure. Can J Earth Sci 22:1813–1817.

Witmer LM. 1995. The extant phylogenetic bracket and the importance of reconstructing soft tissues in fossils. In: Thomason JJ, editor. Functional morphology in vertebrate paleontology. Cambridge, UK: Cambridge University Press.

Woo S, Maynard J, Butler D. 1987. Ligament, tendon, and joint capsule insertions to bone. In: Woo S., Buckwalter JA, editors. Injury and repair of the musculoskeletal soft tissues. Park Ridge, IL: American Academy of Orthopaedic Surgeons.

Yalden DW. 1971. The functional morphology of the carpus in ungulate animals. Acta Anat 78:461–487.